

Alkyne Activation in the Diversity Oriented Synthesis of sp^2 -Rich Scaffolds: A Biased Library Approach for Targeting Polynucleotides (DNA/RNA)

Shuqi Chen,^[a] Daniel L. Priebbenow,^[a] Julie Somkhit,^[a] Carmen V. Scullino,^[a] Keli Agama,^[b] Yves Pommier,^[b] and Bernard L. Flynn^{*[a]}

Abstract: Polynucleotides, DNA and RNA (mRNA and non-coding RNAs) are critically involved in the molecular pathways of disease. Small molecule binding interactions with polynucleotides can modify functional polynucleotide topologies and/or their interactions with proteins. Current approaches to library design (lead-like or fragment-like libraries) are based on protein-ligand interactions and often include careful consideration of the 3-dimensional orientation of binding motifs and exclude π -rich compounds (polyfused aromatics) to avoid off-target R/DNA interactions. In contrast to proteins, where π,π -interactions are weak, polynucleotides can form

strong π,π -interactions with suitable π -rich ligands. To assist in designing a polynucleotide-biased library, a scaffold-divergent synthesis approach to polyfused aromatic scaffolds has been undertaken. Initial screening hits that form moderately stable polynucleotide-ligand-protein ternary complexes can be further optimized through judicious incorporation of substituents on the scaffold to increase protein-ligand interactions. An example of this approach is given for topoisomerase-1 (TOP1), generating a novel TOP1 inhibitory chemotype.

Introduction

Polynucleotides, DNA and RNA, play critical roles in protein expression and are involved in effectively all molecular pathways of disease.^[1–7] While most small-molecule drug discovery efforts are directed to the design of ligands for the encoded protein products of DNA and RNA, significant potential lies in the direct targeting of polynucleotides and the protein-polynucleotide complexes involved in the decoding process (transcription and translation) and/or in epigenetic modifications to the code.^[1–7] Over the last twenty years, diversity-oriented synthesis (DOS) and fragment-based drug discovery (FBDD) have emerged as successful methods for accessing suitable screening sets for phenotypic and target-based drug discovery.^[8–13] The library design principles employed in these DOS and FBDD efforts, such as fraction- sp^3 (Fsp³) and lead-

likeness, have been principally developed with protein targets in mind.^[8–13] In contrast to proteins, where π,π -interactions are weak, the binding of small molecules to polynucleotides often involves strong π,π -interactions, favoring sp^2 -rich molecules.^[1,14,15] This is reflected in nature, where a diverse array of sp^2 -rich bioactive secondary metabolites has been identified that make strong π,π -interactions with polynucleotides, for example, DNA intercalators camptothecin **1** and berberine **2** (Figure 1).^[16–18] Natural products **1** and **2** and their synthetic analogues, such as ARC111 **3** and indenoisoquinolines LMP744 **4**, target DNA-topoisomerase I (TOP1) cleavage complexes (TOP1ccs), disrupting DNA replication and transcription.^[16–21] Transcriptional modification has also been achieved through the targeting of other DNA-protein complexes (e.g., DNA complexes with transcription factors, RNA polymerases and epigenetic modulators) or of functional DNA topologies (e.g., Z-DNA and G-quadruplexes).^[22–27] These DNA-small molecule binding events can lead to changes in the expression of mRNAs and of non-coding RNAs (e.g., micro-RNAs), leading to down-stream changes in protein expression and cellular phenotype. Direct targeting of RNAs with small molecules is also an area of intense interest.^[28] A notable example is the recently approved drug for spinal muscular atrophy, risdiplam **5**, that binds to the mRNA encoding the dysfunctional survival motor neuron 2 (SMN2) protein and promotes read-through of a stop codon to give more functional SMN protein.^[29,30] Another example is the screening hit **6**, which selectively binds to a G-quadruplex within the mRNA encoding the oncogenic N-Ras protein, suppressing its translation.^[31] These and the many other examples of sp^2 -rich compounds targeting polynucleotides indicate that DOS approaches directed to diverse sets of sp^2 -

[a] S. Chen, D. L. Priebbenow, J. Somkhit, C. V. Scullino, B. L. Flynn
Monash Institute of Pharmaceutical Sciences, Monash University
381 Royal Parade, Parkville, VIC 3052 (Australia)
E-mail: bernard.flynn@monash.edu

[b] K. Agama, Y. Pommier
Laboratory of Molecular Pharmacology & Developmental Therapeutics
Branch
Center for Cancer Research, National Cancer Institute, NIH
Bethesda, MD 20892, (United States)

Supporting information for this article is available on the WWW under
<https://doi.org/10.1002/chem.202201925>

© 2022 The Authors. Chemistry - A European Journal published by Wiley-VCH GmbH. This is an open access article under the terms of the Creative Commons Attribution Non-Commercial NoDerivs License, which permits use and distribution in any medium, provided the original work is properly cited, the use is non-commercial and no modifications or adaptations are made.

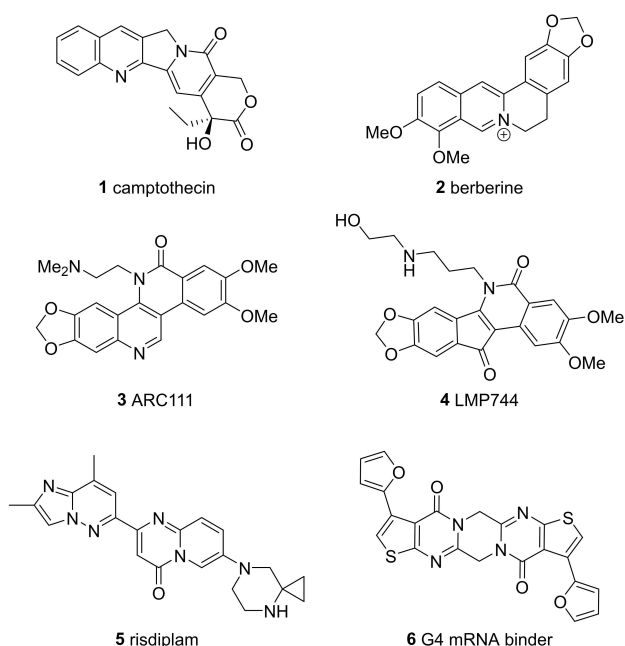


Figure 1. Polynucleotide targeting agents.

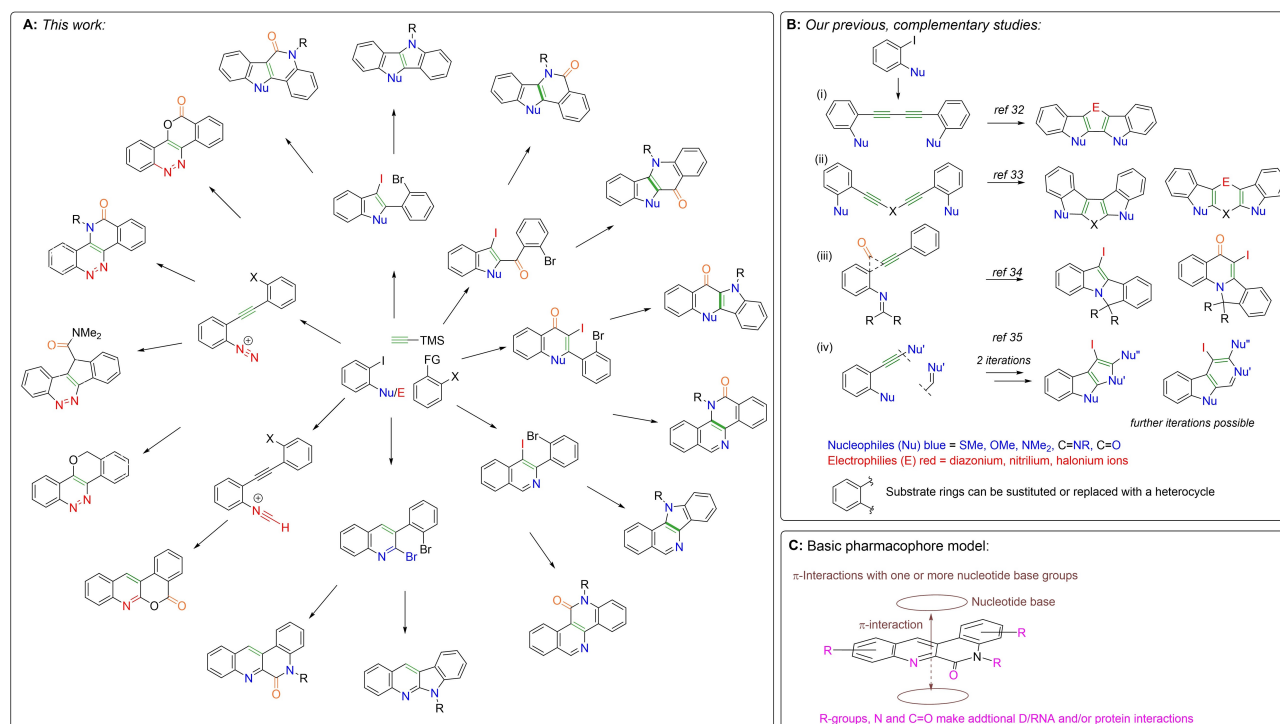
rich scaffolds could prove useful in the discovery of new therapies based on targeting polynucleotides (DNA, mRNA, micro-RNA and other non-coding RNAs).

In this study, we describe a scaffold-divergent approach to heteroacenes based on electrophilic cyclization of alkynes

(Scheme 1A). The divergent methods employed in this work are complemented by several recent studies that we have undertaken to attain other heteroacene scaffolds from the same substrates (Scheme 1B).^[32–35] By analogy with “fragment-growth” approaches in FBDD,^[36–40] we anticipate that by initially establishing positive π,π -interactions with nucleotide bases, the polynucleotide binding fragment can be “grown” through SAR- and/or structure-guided approaches to make additional interactions with a protein binding partner (Scheme 1C). To exemplify this possibility we have biased our new scaffolds towards TOP1 inhibitory activity through incorporation of *N,N*-dimethylaminoethylene group [Scheme 1A, R = $-(\text{CH}_2)_2\text{NMe}_2$] present in a number of non-camptothecin TOP1 inhibitors, such as 3 and have identified a novel TOP1 inhibitor class.^[19] Moreover, we anticipate this DOS method could be employed in the discovery of new polynucleotide targeting agents with novel modes of action.

Results and Discussion

The electrophilic cyclization of alkynes has emerged as a functional group tolerant method of synthesis for a range of aromatic heterocycles and carbocycles.^[41–48] In this work, we have sought to achieve a diversification of a discrete set of substrates by modifying the nature of the nucleophile (Nu) or electrophile (E) and X (X = halide, amide, or ester) (Scheme 1A). For reactions proceeding through diazonium and nitrilium intermediates one-step bicyclization methods have been developed (Scheme 1). For those proceeding through a dihalide

Scheme 1. Scaffold-morphing approach to access sp^2 -rich scaffolds.^[32–35]

intermediate (I/Br or Br/Br), second ring closure can potentially be achieved through various methods.^[49–51] In this work we have employed an Ullmann coupling cyclization (UCC) **7**→**8** and a Pd-mediated carboxyamidation cyclization (PdCC) sequence **7**→**9a,b**→**10a,b** (Schemes 1 and 2). The PdCC can be achieved in a single operation using catalytic Pd(OAc)₂ and CO_(g) (PdCC¹), however, in cases where this stalls at the amide **9a,b**, Ullmann conditions (UCC) are employed to complete cyclization to **10a,b** (PdCC²). The regioselectivity of this process can be controlled based on the relative reactivity of I and Br to Pd-insertion, i.e., **7** (X=I, Y=Br) gives lactam **10a** and **7** (X=Br, Y=I) gives lactam **10b**. In this work, all UCC and PdCC reactions have been performed with 1,1-dimethylethylenediamine (DMD), to give **8–10** R=(CH₂)₂NMe₂, so as to bias the product towards TOP1 inhibition. This R-group can be further diversified in a broader screening set.

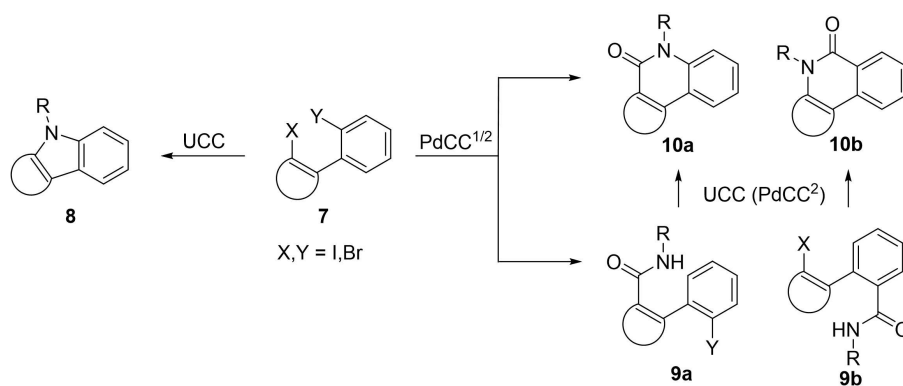
Our first series of heteroacenes incorporated a strategy to optionally diversify the positioning of a carbonyl atom in related scaffolds **16a,b**, **17a,b**, **19a,b**, **23** and **27** (Scheme 3, Part A). Sequential Sonogashira coupling of terminal alkynes **12a,b** (accessed from **11a,b**) with either 1,2-diiodobenzene or 1-bromo-2-iodobenzene furnished substrates **13a,b** and **14a,b** in good to excellent yields (64%–100%). Iodocyclization of bromides **13a,b** with molecular iodine furnished iodo-bromo compounds **15a,b** (78%–95%). The bromocyclization of iodides **14a,b** required greater experimentation, though the best yields were obtained using CuBr₂ for the methylsulfide **14a** and *N*-methylpyrrolidin-2-one hydrotribromide (MPHT) for the methyl ether **14b** to give corresponding bromo-iodo compounds **18a,b** (42%–81%).^[52] UCC and PdCC^{1/2} of **15a,b** with DMD gave pyrroles **16a,b** (29%–42%) and lactams **17a,b** (43%–46%), respectively. Attempted formation of the regioisomeric lactams **19a,b** through PdCC² of **18a,b** with DMD was successful for the thiopheno system **18a**→**19a** (63%) but stalled at the amide stage for furano system **18b** (amide not shown), which could not be ring-closed to **19b**, reflecting a limitation in the method for scaffold **19** (Nu=O).

Further transposing of the carbonyl was achieved in the synthesis of scaffold analogues **23** and **27** (attempted for Nu=SMe only). For **23** this involved reaction of lithiated alkyne **12a**

with Weinreb amide **20** to give propynone **21** (71%), which underwent efficient iodocyclization to **22** (100%) and UCC with DMD to give **23** (36%) in modest yield.^[53] For **27**, reaction of lithiated **11a** (Li for I exchange) with propynamide **24** afforded propynone **25** (71%), that underwent iodocyclization to **26** (52%) and UCC with DMD to give **27** (78%). These syntheses required two recent innovations in iodocyclization chemistry.^[53,54] Firstly, the iodocyclization of alkynes with unfavourable electronic bias **21**→**22**, using high iodine concentrations at elevated temperatures.^[53,54] Secondly, *endo/exo* control in the iodocyclization of **25**, where more polar iodonium sources (ICl in CH₃CN) favour 6-*endo* iodocyclization and iodine in CH₂Cl₂ favors 5-*exo* cyclization.^[54] It should be noted that the iodocyclization of alkynes bearing the carbonyl on the carbon undergoing the nucleophilic attack, as in **21**→**22**, cannot be achieved for furans and indoles (i.e., where SMe is replaced with OMe and NMe₂).^[53] However, 6-*endo* iodocyclization is highly favoured related substrates to **25**, where SMe is replaced with OMe or NMe₂,^[55,56] suggesting plausible access to chromanone and quinolone equivalents to **27**.

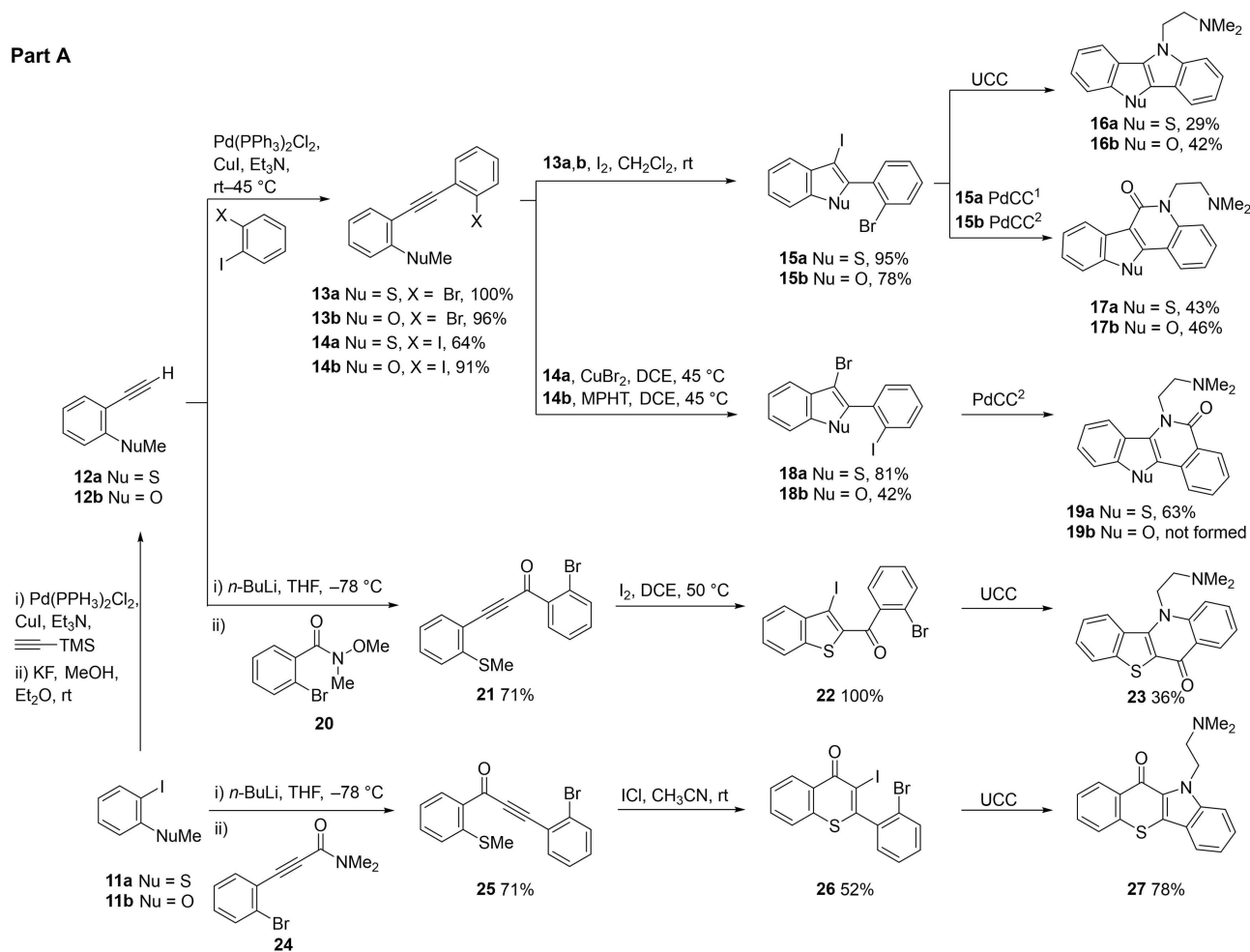
In Scheme 3(Part B), we exemplified two other modes of divergent heteroacene synthesis. Firstly, the 1,2-dihalobenzene used to access **13–14a,b** can be replaced with 2,3-dibromothiophene (and potentially other dihaloheterocycles) to progress through the Sonogashira coupling (**28**, 58%), iodocyclization (**29**, 97%) and PdCC² sequence to give the thiophene analogue of **17a**, **30** (44%). In the second example, another latent nucleophile (Sme) is introduced onto the alkyne **12a** to give **31** (96%), which enables a sequence of iodocyclization (**32**, 91%), Sonogashira coupling and iodocyclization (**34**, 48%), followed by PdCC² to give **35** (57%).^[35]

We next investigated the construction of a series of equivalent pyridyl analogues **40**, **41**, and **43** (Scheme 4, Part A). This approach centered on the halocyclization of imines **38a,b**. The synthesis of **38a,b** involved Sonogashira coupling of 2-iodobenzaldehyde **36** with bromoethynylbenzene **33** to give **37** (92%) followed by Schiff base condensation with MeONH₂ (Method A) to give **38a** (94%) or *t*-BuNH₂ (Method B) to give **38b** (not isolated). Bromocyclization of **38a** was achieved using the method previously described by Yu et al.^[57] employing

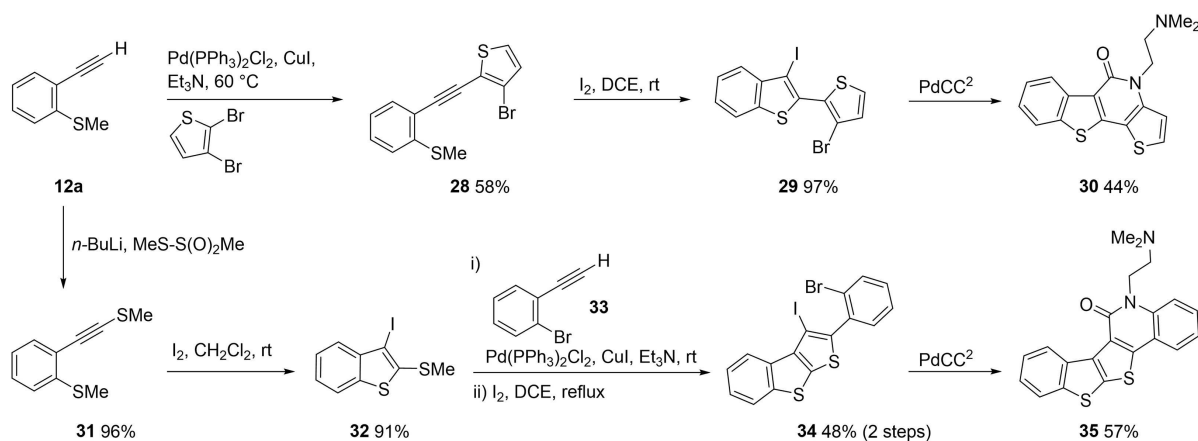


Scheme 2. Late-stage ring closure of dihalides **7**. Ullmann coupling cyclization (UCC): R-NH₂, CuI 20–40 mol%, K₃PO₄, *n*-BuOH, ethylene glycol. Pd-mediated carboxyamidation cyclization-1 (PdCC¹): R-NH₂, Pd(OAc)₂ 10 mol%, PPh₃, CO_(g), Et₃N, NMP. Pd-mediated carboxyamidation cyclization-2 (PdCC²): as for PdCC¹ then UCC

Part A

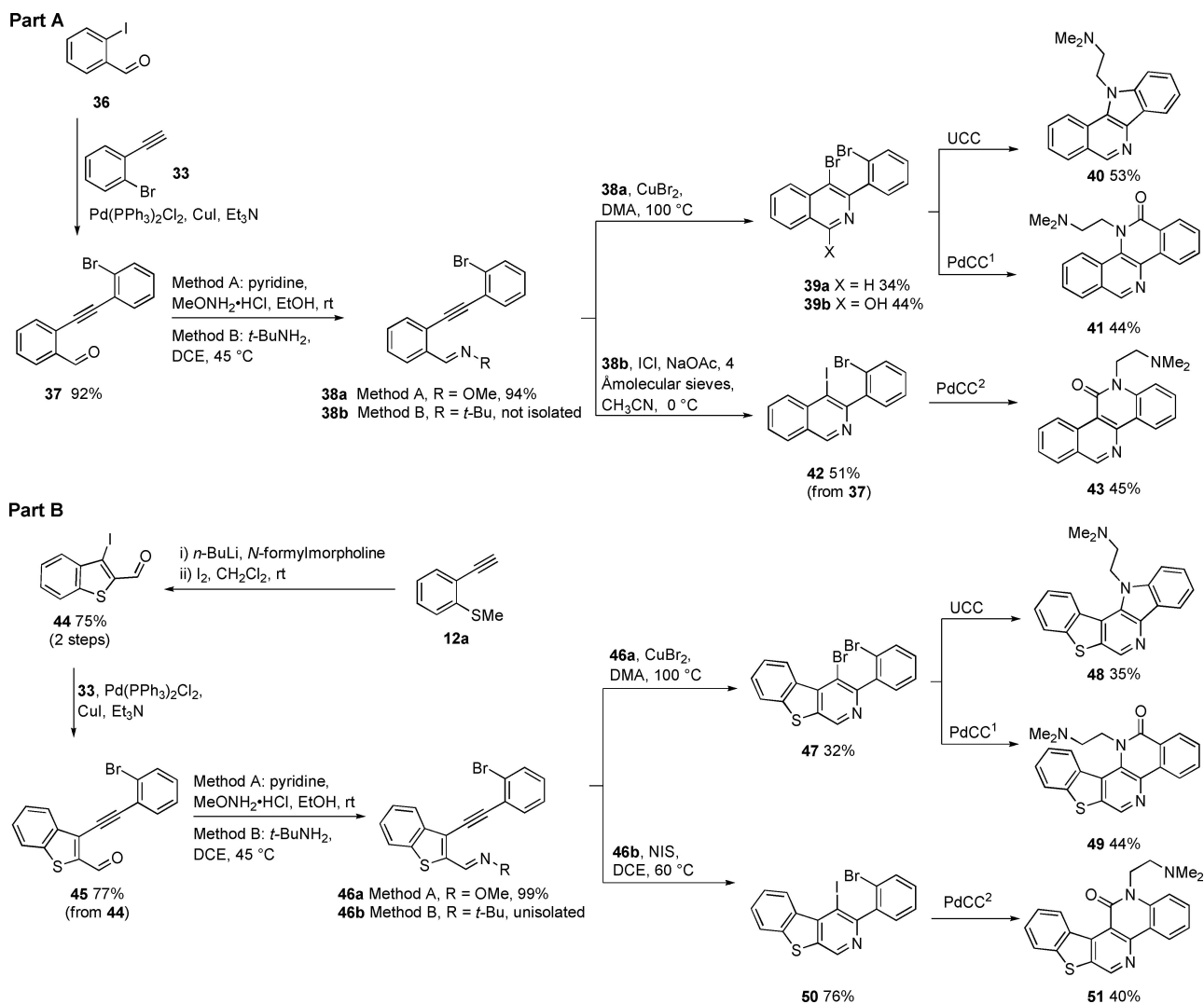


Part B

Scheme 3. Preparation of **16a,b**, **17a,b**, **19a,b**, **23**, **27**, **30** and **35**^[53]

CuBr₂ in DMA at 100 °C, giving **39a** (34%). The yield of this reaction was limited by a competing oxidative-cyclization to give lactam **39b** (44%) as the major by-product.^[58] Oxime **38a** could not be iodocyclized, though the corresponding *t*-Bu-aldimine **38b** could be by employing ICl in CH₃CN with a weak base (NaOAc) to give product **42** (51%).^[59] UCC of dibromide

39a with DMD gave the heterotetracene **40** (53%). PdCC¹ of dibromide **39a** with DMD proved surprisingly regioselective, favoring lactam **41** (44%) as the major product (no regioisomeric lactam could be detected).^[60] A possible explanation for this regioselectivity is that under the thermal reaction conditions (80 °C in *N*-methyl-2-pyrrolidone) nucleophilic aromatic

Scheme 4. Preparation of **40**, **41**, **43**, **48**, **49**, and **51**.^[53]

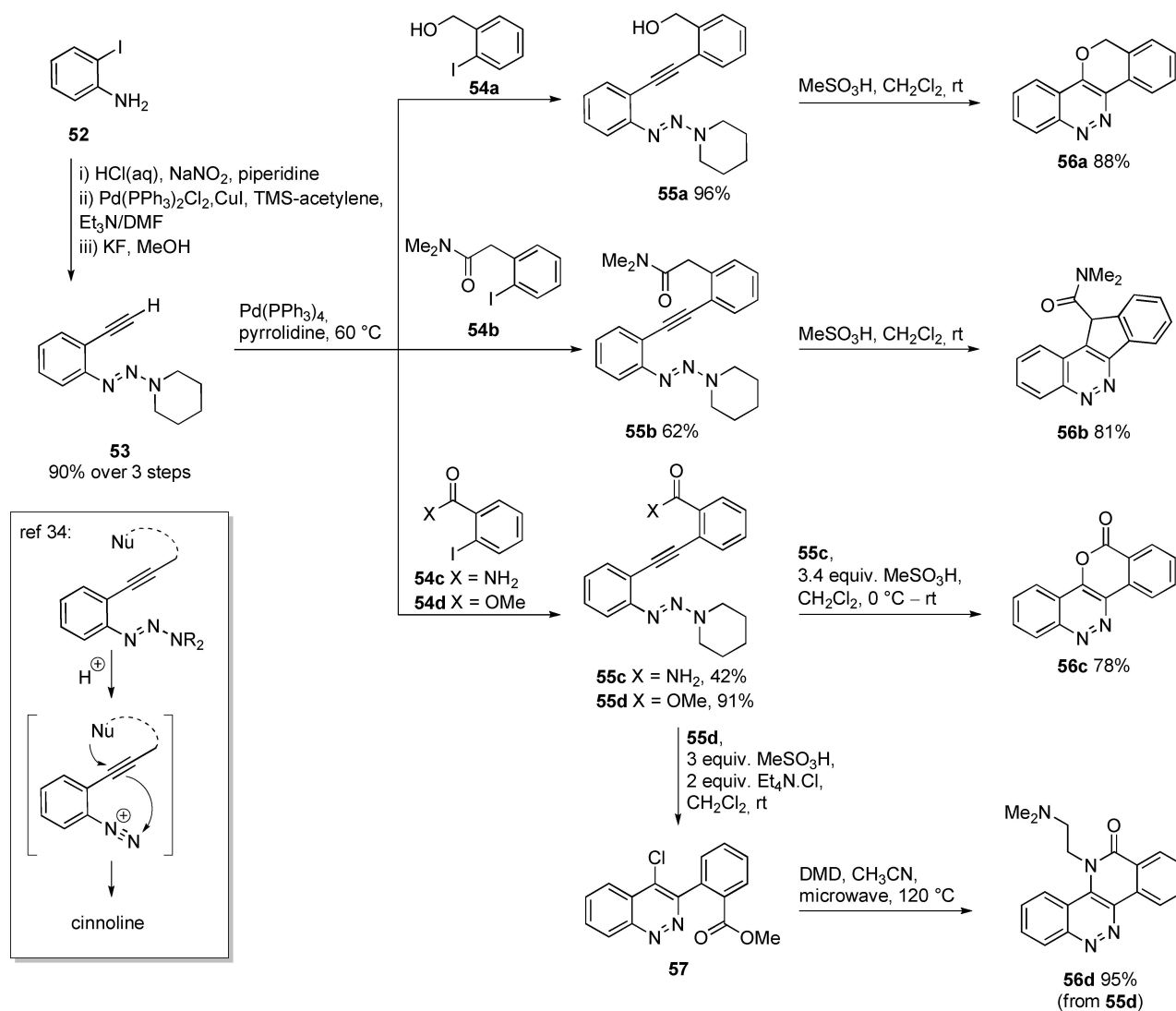
substitution of the bromo group on the isoquinoline precedes Pd-mediated carbonylative ring closure onto the bromophenyl ring. This regioselectivity is reversed in the PdCC² of the iodobromo substrate **42** with DMD, giving **43** (45%). In this case, Pd-mediated carboxyamidation with DMD precedes ring closure onto the bromophenyl, in a separate UCC step.

In Scheme 4(Part B), alkyne **12a** was converted into 3-iodobenzo[*b*]thiophene-2-carbaldehyde (**44**) by formylation and iodocyclization. Iodoaldehyde **44** was then subject to a related series of reactions to those used in Part A to generate a series of thiopheno-fused systems **48**, **49** and **51**.^[53]

In earlier work, we had demonstrated the utility of triazenes to operate as masked diazoniums that could be unmasked by acid in the presence of a nucleophile Nu (tethered or untethered) to give a cinnoline (Scheme 5 Box).^[34] In this study, we exploited this chemistry in the rapid assembly of a series of cinnolines **56a–d** from 2-iodoaniline **52** (Scheme 5). Terminal alkyne **53** was prepared in three steps, involving diazotisation and triazene formation, followed by Sonogashira coupling with

TMS-acetylene and deprotection. A Cu-free Sonogashira coupling was employed to couple alkyne **53** to iodobenzenes **54a–d**, giving tolans **55a–d** (42%–96%). Treatment of tolans **55a–c** with MeSO₃H unmasked the diazonium cation and induced electrophilic co-cyclization to give **56a–c**. Treatment of the ester **55d** with MeSO₃H in the presence of tetraethylammonium chloride gave a chlorocinnoline **57** (unpurified). Reaction of **57** with DMD at elevated temperature afforded **56d** (a previously described TOP1 inhibitor)^[61] through a domino nucleophilic aromatic substitution/lactamization sequence in excellent yield (95%).

Given the success of the diazonium cyclizations to give cinnolines, we proposed to explore the related cyclization on nitrilium ion **62** to give **63** and **64** (Scheme 6). Sonogashira coupling of 2-iodophenylformamide **58** to alkynes **59** and **33** gave tolans **60a** and **60b**, respectively (66–67%). Reaction of **60a** with Burgess reagent and of **60b** with POCl₃ and diisopropylethylamine (DIPEA) gave rise to the isocyanides **61a** and **61b**, respectively. Both isocyanides **61a,b** were stable in

Scheme 5. Preparation of 56a–d^[34]

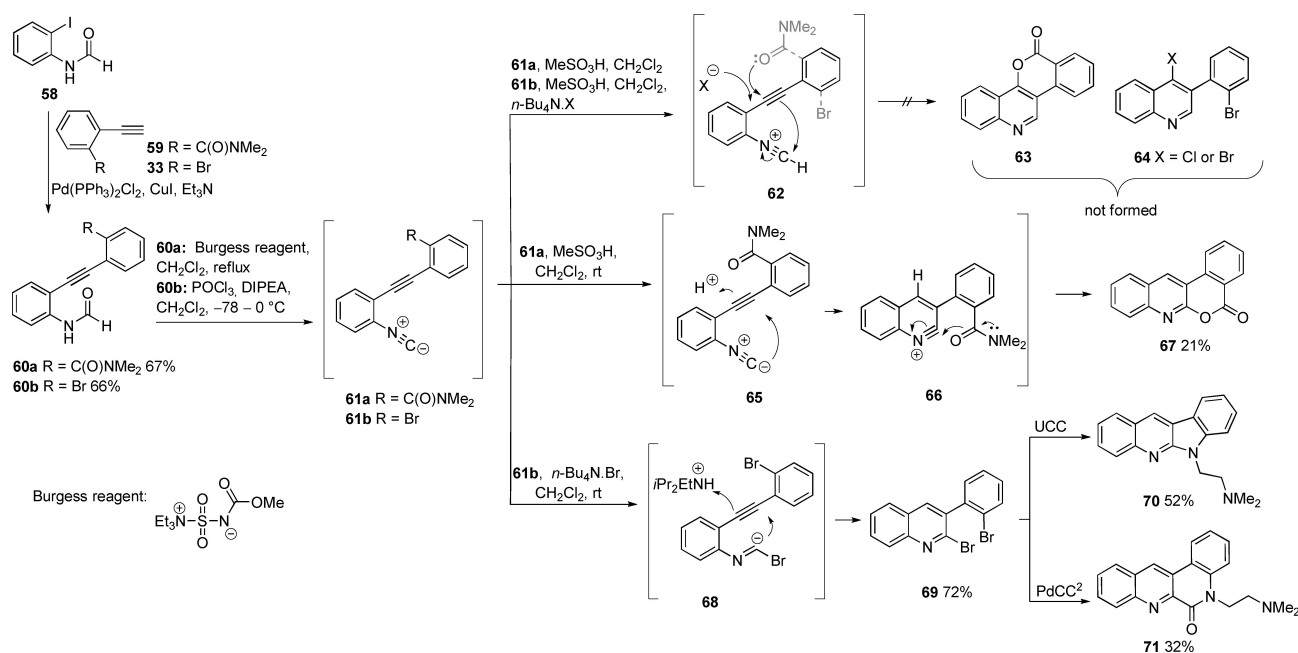
solution (¹H NMR), but reverted to the formamides **60a,b** upon attempted extractive work up, consequently, they were not isolated but used directly in the next reaction. Attempted protonation and cyclization of **61a** and **61b** to quinolines **63** and **64** respectively, via nitrilium ion **62** failed. Rather, **61a** gave the regioisomeric quinoline **67** (21% from **60a**) and **61b** reverted to the formamide **60b**. Bromocyclization of **61b** to give **69** (72%) was achieved upon addition of *n*-Bu₄N.Br without acid, in a process previously described by Mitamura et al.^[62] This involves nucleophilic cyclization of a bromide adduct ion **68** with concomitant protonation by residual diisopropylethylammonium ion (from isonitrile formation). Ring closure of dibromide **69** under UCC and PdCC² conditions gave **70** (52%) and **71** (32%), respectively.

Finally, since **19a** (Scheme 3) proved to be active as a TOP1 inhibitor (see below), we also prepared an analogue **77** (Scheme 7) that bears the additional TOP1 protein binding methoxy and methylenedioxy groups seen in **3** and **4**

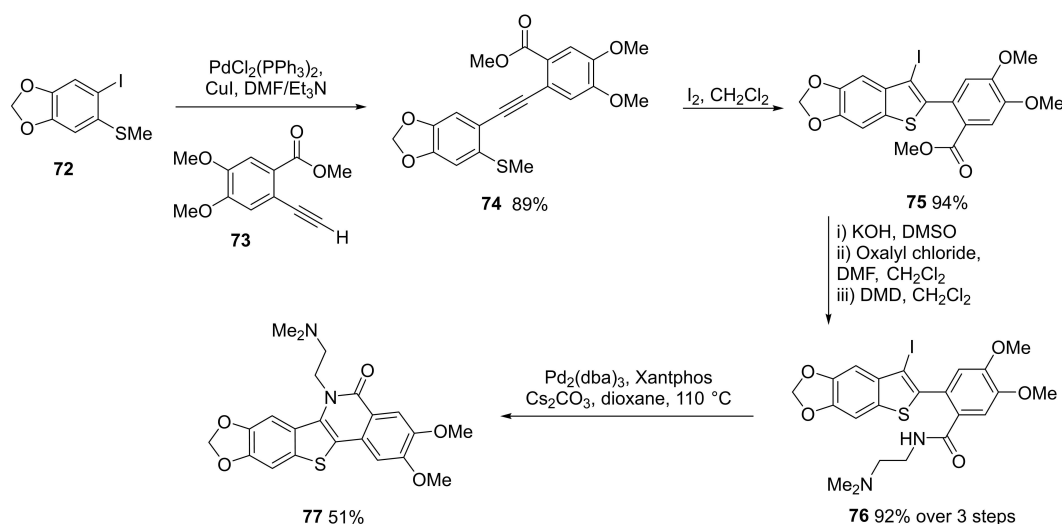
(Scheme 1).^[17] Sonogashira coupling of aryl iodide **72** and arylalkyne **73** afforded tolan **74** (89%). Iodocyclization of **74** proceeded chemoselectively through the methylsulfide (and not the ester) to give benzo[*b*]thiophene **75** (94%). The ester was efficiently converted to the amide **76** (92% over 3 steps) and cyclized under Buchwald-Hartwig conditions to furnish the target compound **77** (51%).

Topoisomerase I inhibitory activity

TOP1 plays a key role modifying and maintaining DNA topology during cellular replication and transcription.^[17,63] TOP1 inhibitors, such as **1–4**, exert their cytotoxic effect on cancer cells by binding to TOP1/DNA cleavage complexes (TOP1cc), forming stable ternary complexes that collide with replication forks leading to DNA damage and apoptosis.^[17,21] TOP1 inhibitors also influence transcription, for example, in hypoxic cancer cells



Scheme 6. Preparation of 67, 70 and 71.



Scheme 7. Preparation of fully decorated compound 77.

compounds **1** and **2** selectively suppress the expression of hypoxia inducible factor HIF-1 α , which is a driver of tumour progression.^[64–66] In this scenario, inhibition of TOP1 increases in the transcription of micro-RNAs, miR-17-5p and miR-155, that promote selective degradation of HIF-1 α mRNA.^[65]

While the purpose of this study has been to develop a DOS of heteroacenes using electrophilic alkyne activation, several scaffolds generated in this work are reminiscent of DNA intercalators that inhibit TOP1, such as **2–4** (Figure 1).^[17,67] To further bias these scaffolds to interact with TOP1cc we included the *N,N*-dimethylaminoethylene group in ARC111 to many of the synthesised compounds.

All new scaffolds (Figure 2) were tested for TOP1 inhibition at 100, 10, 1, and 0.1 μ M in a TOP1-mediated DNA cleavage assay.^[68] This assay uses 3'-radiolabeled DNA substrates to identify compounds that stabilise TOP1ccs. Active TOP1 inhibitors were also tested for cytotoxicity towards prostate cancer PC3 cells. Two of the scaffolds tested, **78** and **79**, were generated using our previously described double-electrophilic cyclization chemistry, which complements this work (Scheme 1Bii).^[32,33] Of all the scaffolds studied only **19a** and **56d** showed significant TOP1 inhibition in a dose-dependent manner (Figure 3).^[69]

Aspects of the scaffold SAR are quite steep. For example, replacement of one nitrogen in cinnoline **56d** for a CH-group in

Compounds generated in this study:

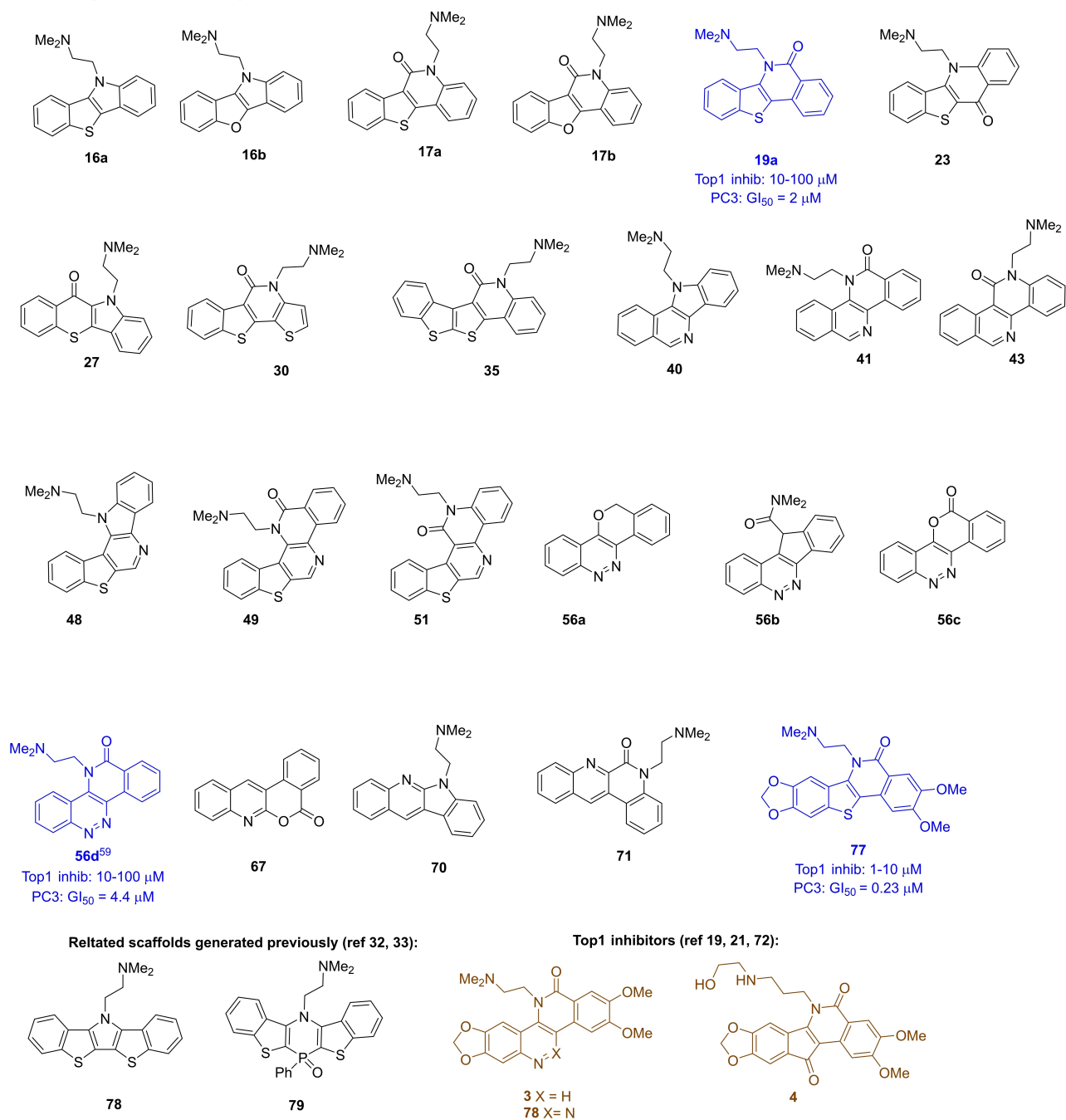


Figure 2. Compounds evaluated for TOP1 activity. Active compounds from this work shown in blue (see also Figure 3), known actives shown in brown.^[19,21,32,33,72]

isoquinoline **41** led to a complete loss in activity, as did a swap in the location to the carbonyl in **19a** vs. **17a**. The carbonyl and ring heteroatoms of other related TOP1 inhibitors are known to facilitate protein-binding within the TOP1cc. Crystal structures of camptothecin and non-camptothecin ligands bound to the TOP1cc reflect a similar scenario to that depicted in Scheme 1C, where the π -rich TOP1 inhibitor is sandwiched (intercalated) between two sets of DNA base pairs through π , π -interactions and the ring-heteroatoms, carbonyls and other substituents at

the “edge” of this sandwich make important interactions with the TOP1 protein amino-acid sidechains.^[70,71] Accordingly, while the polyaromatic core of **56d**, **41**, **19a** and **17a** makes important π , π -interactions with DNA in the Top1cc, small differences in the location of the edge-groups has significant impact on overall stability of the ternary complex and associated potency. Other substituents attached to this core also impact potency, presumably through ligand-protein interactions. The inactivity of **56c** compared to **56d** suggests that

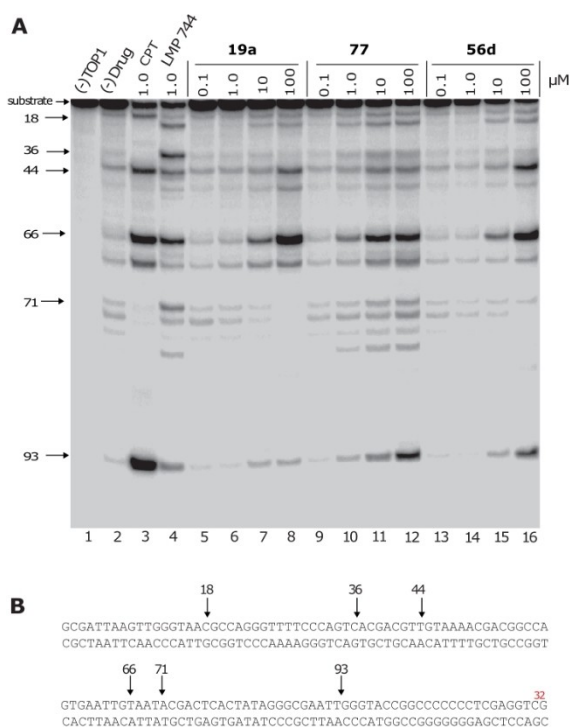


Figure 3. A. Representative gel of the TOP1-mediated DNA cleavage assay. From left to right: Lane 1, DNA alone; lane 2, DNA and TOP1 without drug; lane 3, DNA and TOP1 with CPT (1 μM); lane 4, DNA and TOP1 with LMP744 (1 μM); lanes 5–16, DNA and TOP1 with the tested compounds at 0.1, 1.0, 10, and 100 μM concentrations, respectively. The arrows and numbers at left indicate the cleavage site positions. LMP744 is the positive non-camptothecin indenoisoquinoline control. B. Sequence of the 3'- ^{32}P -labelled 117-bp DNA (labeled Guanine in red) with the indicated TOP1 cleavage site positions.^[68]

the ethylene linked dimethylamino group may also make important protein interactions in the ternary TOP1cc, as do the methylenedioxy and/or methoxy groups present in **3**, which is approximately 10-fold more potent than **19a** in terms of TOP1

inhibition.^[70] The relative potency of **19a**, **56d**, and **77** as TOP1 inhibitors is reflected in their inhibition of the PC3 cancer cell growth: **19a** \approx **56b** < **77** (Figure 4).

Conclusion

A scaffold-divergent synthesis strategy for the generation of a sp^2 -rich polynucleotide-biased fragment library has been devised based on the electrophilic cyclization of alkynes (Scheme 2). Scaffold modifications include the use of intermolecular and intramolecular electrophiles and variations in the nature of the second (dihalide) ring closure (Schemes 2–6). The iterative use of halocyclization further extends the range heteroacene scaffolds that can be accessed (Scheme 3 Part B and Scheme 4 Part B). These methods are yet further complemented by our other heteroacene syntheses using electrophilic cyclization (Scheme 1B).^[32–35] The methods are also applicable to the generation of more substituted systems for further library diversification and/or lead optimisation (Scheme 7). The small library of scaffolds generated to date has proven useful in identifying novel TOP1 inhibitors, targeting the TOP1cc. Our group is currently engaged in further characterizing the interactive capacity of the new scaffolds for polynucleotides and further diversifying the library for target-based and phenotypic screening.

Experimental Section

General procedure A (Sonogashira coupling)

For the synthesis of alkynes **13a,b**, **14a,b**, **28**, **37**, **45**, **60a,b**, and **74**: The respective 2-iodobenzene was dissolved in Et_3N (0.2 M) in a dry round-bottom flask (RBF), followed by addition of CuI (4–6 mol%) and $\text{Pd}(\text{PPh}_3)_2\text{Cl}_2$ (2–3 mol%). The RBF was then degassed and backfilled with $\text{N}_2(\text{g})$ three times. Finally, a solution of the terminal alkyne (1.2 equiv.) in Et_3N (1 M) was added dropwise under

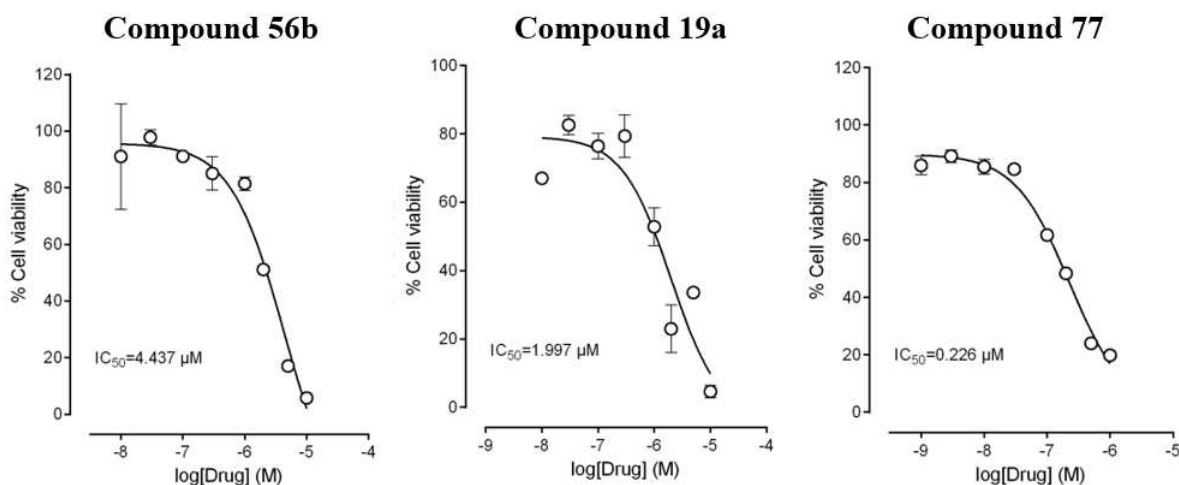


Figure 4. PC3 cell viability was measured using an MTS colorimetric assay at eight concentrations (10^{-8} – 10^{-4} M, $n=3$ per concentration) and is given as the concentration required to inhibit 50% of cell growth (IC_{50}).^[73]

an N₂(g) atmosphere. The reaction mixture was stirred at rt to 60 °C overnight. On completion, the suspension was filtered through Celite® and rinsed with Et₂O. The organic extract was washed with H₂O twice and with brine twice, dried over anhydrous MgSO₄, filtered and concentrated under reduced pressure. The crude product obtained was purified by flash column chromatography to yield the desired alkyne.

General procedure B (Cu-free Sonogashira coupling)

For the synthesis of alkynes **55 a–d**: **54 a–d** was dissolved in pyrrolidine (0.5 M), followed by addition of Pd(PPh₃)₄ (5 mol%). The RBF was degassed and backfilled with N₂(g) for three times. Finally, a solution of **53** (1.5 equiv.) in pyrrolidine (3 M) was added dropwise under N₂(g) atmosphere. The reaction mixture was heated at 60 °C for 4–16 h. On completion, the suspension was filtered through Celite® and rinsed with EtOAc. The organic extract was washed with H₂O three times, dried over anhydrous MgSO₄, filtered and concentrated under reduced pressure. The crude product obtained was purified by flash column chromatography (1:1 hexanes:EtOAc) to yield the desired alkynes **55 a–d**.

General procedure C (Sonogashira Coupling-Desilylation)

For the synthesis of alkynes **53**, **59**, and **73**: The respective 2-iodobenzene was dissolved in Et₃N (0.2 M) in a dry round-bottom flask (RBF), followed by addition of CuI (4–6 mol%) and Pd(PPh₃)₂Cl₂ (2–3 mol%). The RBF was then degassed and backfilled with N₂(g) three times. Finally, trimethylsilylacetylene (1.2 equiv.) was added dropwise under an N₂(g) atmosphere. The reaction mixture was stirred at rt overnight. On completion, the suspension was filtered through Celite® and extracted with Et₂O twice and washed with H₂O twice and with brine twice. The combined organic extracts were dried over anhydrous MgSO₄, filtered, and concentrated under reduced pressure. The crude product was purified by a silica plug (100% hexanes) to yield the TMS-protected terminal alkyne, which was then dissolved in MeOH/Et₂O (2:1, 0.2 M), followed by addition of K₂CO₃ (1–2 equiv.). The reaction mixture was stirred at rt overnight. On completion, the mixture was concentrated to a residue, taken up in Et₂O, washed with H₂O twice and with brine twice. The organic extract was dried over anhydrous MgSO₄, filtered, and concentrated to yield the desired terminal alkyne, which was directly used in the next step without further purification.

General procedure D (Iodocyclization)

For the synthesis of iodides **15 a,b**, **22**, **29**, **34**, **44**, **75**: I₂ (1.2–3 equiv.) was added to a stirred solution of the respective alkyne substrate in dry CH₂Cl₂ (0.2 M) under an N₂(g) atmosphere. The reaction mixture was stirred at rt for 1–18 h. On completion, the reaction mixture was quenched with saturated Na₂S₂O₃ solution and extracted with CH₂Cl₂ twice. The combined organic extracts were washed with H₂O twice and with brine twice, dried over anhydrous MgSO₄, filtered, and concentrated under reduced pressure to yield the desired iodocyclized product.

General UCC procedure

For the final ring closure of **15 a,b**, **22**, **26**, **39 a**, **47**, **69**: In a dry RBF, the respective dihalide was dissolved in dry *n*-butanol or DMF (0.1–0.2 M). K₃PO₄ (4 equiv.), ethylene glycol (12 equiv.), 1,1-dimethylethane-1,2-diamine (DMD) (15 equiv.) and CuI (10–40 mol%) were added sequentially into the flask. The RBF was degassed and

backfilled with N₂(g) three times, and the reaction mixture was heated at 80–110 °C. On completion, the reaction mixture was cooled down to rt, quenched with saturated NH₄Cl solution and extracted with EtOAc twice. The combined organic extracts were washed with H₂O three times and with brine twice, dried over anhydrous MgSO₄, filtered, and concentrated under reduced pressure. The crude product obtained was purified by flash column chromatography to yield the desired alkyne.

General PdCC¹ procedure

For the final ring closure of **15 a**, **39 a**, **47**: The respective dihalide, Pd(OAc)₂ (10 mol%), CuI (10 mol%), PPh₃ (1.5 equiv.), DMD (15 equiv.), Et₃N (2 equiv.) and dry NMP (0.1–0.15 M) was added to a dry RBF. The RBF was degassed and backfilled with CO(g) for three times, the reaction mixture was then heated at 80 °C for 15–49 h under CO(g) atmosphere. On completion, the reaction mixture was cooled down to rt, quenched with saturated NH₄Cl solution and extracted with EtOAc twice. The combined organic extracts were washed with H₂O three times and with brine twice, dried over anhydrous MgSO₄, filtered, and concentrated under reduced pressure. The crude product obtained was purified by flash column chromatography to yield the desired final product.

General PdCC² procedure

For the final ring closure of **15 b**, **18 a**, **29**, **34**, **42**, **50**, **69**: Step 1: use General PdCC¹ Procedure to form the secondary amide; step 2: use a modified UCC Procedure to close the ring and form final products (use *N,N,N',N'*-tetramethylethane-1,2-diamine (TMD) in lieu of DMD).

Supporting Information

TOP1-mediated DNA cleavage assay gel of tested compounds, PC3 cell viability assays, Experimental procedures and characterization data, ¹H and ¹³C NMR Spectral Data

Acknowledgements

Open Access publishing facilitated by Monash University, as part of the Wiley - Monash University agreement via the Council of Australian University Librarians.

Conflict of Interest

The authors declare no conflict of interest.

Data Availability Statement

The data that support the findings of this study are available from the corresponding author upon reasonable request.

Keywords: alkynes · electrophilic cyclization · polynucleotides · RNA/DNA · topoisomerase

- [1] J. Sheng, J. Gan, Z. Huang, *Med. Res. Rev.* **2013**, *33*, 1119–1173.
- [2] R. R. Breaker, G. F. Joyce, *Chem. Biol.* **2014**, *21*, 1059–1065.
- [3] C. M. Connelly, M. H. Moon, J. S. Schneekloth, *Cell Chem. Biol.* **2016**, *23*, 1077–1090.
- [4] K. D. Warner, C. E. Hajdin, K. M. Weeks, *Nat. Rev. Drug Discovery* **2018**, *17*, 547–558.
- [5] A. M. Alnuqaydan, *Am. J. Transl. Res.* **2020**, *12*, 3531–3556.
- [6] Y. Shao, Q. C. Zhang, *Essays Biochem.* **2020**, *64*, 955–966.
- [7] J. P. Falese, A. Donlic, A. E. Hargrove, *Chem. Soc. Rev.* **2021**, *50*, 2224–2243.
- [8] D. S. Tan, *Nat. Chem. Biol.* **2005**, *1*, 74–84.
- [9] E. Lenci, L. Baldini, A. Trabocchi, *Bioorg. Med. Chem.* **2021**, *41*, 116218.
- [10] C. J. Gerry, S. L. Schreiber, *Nat. Rev. Drug Discovery* **2018**, *17*, 333–352.
- [11] I. Pavlinov, E. M. Gerlach, L. N. Aldrich, *Org. Biomol. Chem.* **2019**, *17*, 1608–1623.
- [12] S. Yi, B. V. Varun, Y. Choi, S. B. Park, *Front. Chem.* **2018**, *6*, 1–8.
- [13] K. T. Mortensen, T. J. Osberger, T. A. King, H. F. Sore, D. R. Spring, *Chem. Rev.* **2019**, *119*, 10288–10317.
- [14] R. Martinez, L. Chacon-Garcia, *Curr. Med. Chem.* **2012**, *12*, 127–151.
- [15] J. Portugal, F. Barceló, *Curr. Med. Chem.* **2016**, *23*, 4108–4134.
- [16] R. P. Hertzberg, M. J. Caranfa, S. M. Hecht, *Biochemistry* **1989**, *28*, 4629–4638.
- [17] Y. Pommier, *Nat. Rev. Cancer* **2006**, *6*, 789–802.
- [18] C. L. Kuo, C. C. Chou, B. Y. M. Young, *Cancer Lett.* **1995**, *93*, 193–200.
- [19] T. K. Li, P. J. Houghton, S. D. Desai, P. Daroui, A. A. Liu, E. S. Hars, A. L. Ruchelman, E. J. LaVoie, L. F. Liu, *Cancer Res.* **2003**, *63*, 8400–8407.
- [20] Y. Pommier, M. Cushman, *Mol. Cancer Ther.* **2009**, *8*, 1008–1014.
- [21] A. Thomas, Y. Pommier, *Clin. Cancer Res.* **2019**, *25*, 6581–6589.
- [22] J. Hagenbuchner, M. J. Ausserlechner, *Biochem. Pharmacol.* **2016**, *107*, 1–13.
- [23] R. Ferreira, J. S. Schneekloth, K. I. Panov, K. M. Hannan, R. D. Hannan, *Cells* **2020**, *9*, 266–289.
- [24] W. Xiao, Q. Zhou, X. Wen, R. Wang, R. Liu, T. Wang, J. Shi, Y. Hu, J. Hou, *Front. Pharmacol.* **2021**, *12*, 702360.
- [25] M. Wang, Y. Yu, C. Liang, A. Lu, G. Zhang, *Int. J. Mol. Sci.* **2016**, *17*, 779.
- [26] I. M. A. del Mundo, K. M. Vasquez, G. Wang, *Biochim. Biophys. Acta Mol. Cell Res.* **2019**, *1866*, 118539.
- [27] H. R. Nasiri, N. M. Bell, K. I. E. Mc Luckie, J. Husby, C. Abell, S. Neidle, S. Balasubramanian, *Chem. Commun.* **2014**, *50*, 1704–1707.
- [28] R. Fan, C. Xiao, X. Wan, W. Cha, Y. Miao, Y. Zhou, C. Qin, T. Cui, F. Su, X. Shan, *RNA Biol.* **2019**, *16*, 707–718.
- [29] N. A. Naryshkin, M. Weetall, A. Dakka, J. Narasimhan, X. Zhao, Z. Feng, K. K. Y. Ling, G. M. Karp, H. Qi, M. G. Woll, G. Chen, N. Zhang, V. Gabbeta, P. Vazirani, A. Bhattacharyya, B. Furia, N. Risher, J. Sheedy, R. Kong, J. Ma, A. Turpoff, C.-S. Lee, X. Zhang, Y.-C. Moon, P. Trifillis, E. M. Welch, J. M. Colacino, J. Babiak, N. G. Almstead, S. W. Peltz, L. A. Eng, K. S. Chen, J. L. Mull, M. S. Lynes, L. L. Rubin, P. Fontoura, L. Santarelli, D. Haehnke, K. D. McCarthy, R. Schmuck, M. Ebeling, M. Sivaramakrishnan, C.-P. Ko, S. v. Paushkin, H. Ratni, I. Gerlach, A. Ghosh, F. Metzger, *Science*. **2014**, *345*, 688–693.
- [30] J. Wang, P. G. Schultz, K. A. Johnson, *Proc. Natl. Acad. Sci. USA* **2018**, *115*, E4604–E4612.
- [31] Y. Katsuda, S. I. Sato, L. Asano, Y. Morimura, T. Furuta, H. Sugiyama, M. Hagihara, M. Uesugi, *J. Am. Chem. Soc.* **2016**, *138*, 9037–9040.
- [32] A. Gupta, B. L. Flynn, *Org. Lett.* **2017**, *19*, 1939–1941.
- [33] A. Gupta, B. L. Flynn, *J. Org. Chem.* **2016**, *81*, 4012–4019.
- [34] A. Goeminne, P. J. Scammells, S. M. Devine, B. L. Flynn, *Tetrahedron Lett.* **2010**, *51*, 6882–6885.
- [35] L. Aurelio, R. Volpe, R. Halim, P. J. Scammells, B. L. Flynn, *Adv. Synth. Catal.* **2014**, *356*, 1974–1978.
- [36] Fragment-growth refers to the incorporation of additional protein-binding groups to a fragment in order to increase affinity and potency for the target, see for examples in references 37–40.
- [37] J. Tsai, J. T. Lee, W. Wang, J. Zhang, H. Cho, S. Mamo, R. Bremer, S. Gillette, J. Kong, N. K. Haass, K. Sproesser, L. Li, K. S. M. Smalley, D. Fong, Y. L. Zhu, A. Marimuthu, H. Nguyen, B. Lam, J. Liu, I. Cheung, J. Rice, Y. Suzuki, C. Luu, C. Settachatgul, R. Shellooe, J. Cantwell, S. H. Kim, J. Schlessinger, K. Y. J. Zhang, B. L. West, B. Powell, G. Habets, C. Zhang, P. N. Ibrahim, P. Hirth, D. R. Artis, M. Herlyn, G. Bollag, *Proc. Natl. Acad. Sci. USA* **2008**, *105*, 3041–3046.
- [38] C. Zhang, P. N. Ibrahim, J. Zhang, E. A. Burton, G. Habets, Y. Zhang, B. Powell, B. L. West, B. Matusow, G. Tsang, R. Shellooe, H. Carias, H. Nguyen, A. Marimuthu, K. Y. J. Zhang, A. Oh, R. Bremer, C. R. Hurt, D. R. Artis, G. Wu, M. Nespi, W. Spevak, P. Lin, K. Nolop, P. Hirth, G. H. Tesch, G. Bollag, *Proc. Natl. Acad. Sci. USA* **2013**, *110*, 5689–5694.
- [39] T. G. Davies, W. E. Wixted, J. E. Coyle, C. Griffiths-Jones, K. Hearn, R. McMenamin, D. Norton, S. J. Rich, C. Richardson, G. Saxty, H. M. G. Willems, A. J. A. Woolford, J. E. Cottom, J. P. Kou, J. G. Yonchuk, H. G. Feldser, Y. Sanchez, J. P. Foley, B. J. Bolognese, G. Logan, P. L. Podolin, H. Yan, J. F. Callahan, T. D. Heightman, J. K. Kerns, *J. Med. Chem.* **2016**, *59*, 3991–4006.
- [40] C. W. Murray, D. R. Newell, P. Angibaoud, *MedChemComm* **2019**, *10*, 1509–1511.
- [41] R. C. Larock, in *Acetylene Chemistry: Chemistry, Biology, and Material Science* (Eds.: F. Diederich, P. J. Stang, R. R. Tykwinski), **2005**, pp. 51–99.
- [42] F. Rodríguez, F. J. Fañanás, *Handbook of Cyclization Reactions, Vol. 2* (Ed.: S. Ma), Wiley-VCH, **2010**, p. 951–990.
- [43] K. Gilmore, I. v. Alabugin, *Chem. Rev.* **2011**, *111*, 6513–6556.
- [44] B. Godoi, R. F. Schumacher, G. Zeni, *Chem. Pharm. Bull.* **2011**, *111*, 2937–2980.
- [45] G. Fang, X. Bi, *Chem. Soc. Rev.* **2015**, *44*, 8124–8173.
- [46] T. Aggarwal, S. Kumar, A. K. Verma, *Org. Biomol. Chem.* **2016**, *14*, 7639–7653.
- [47] A. D. Sonawane, R. A. Sonawane, M. Ninomiya, M. Koketsu, *Adv. Synth. Catal.* **2020**, *362*, 1–32.
- [48] A. R. Pandey, D. K. Tiwari, A. Prakhar, D. P. Mishra, *Monatsh. Chem.* **2022**, *153*, 383–407.
- [49] R. Martin, C. H. Larsen, A. Cuenca, S. L. Buchwald, *Org. Lett.* **2007**, *9*, 3379–3382.
- [50] A. Kicková, B. Horváth, L. Kerner, M. Putala, *Chem. Pap.* **2013**, *67*, 101–109.
- [51] W. Xue, H. Xu, Z. Liang, Q. Qian, H. Gong, *Org. Lett.* **2014**, *16*, 4984–4987.
- [52] M. Jacubert, A. Tikad, O. Provot, A. Hamze, J. D. Brion, M. Alami, *Eur. J. Org. Chem.* **2010**, *2010*, 4492–4500.
- [53] S. Chen, B. L. Flynn, *Aust. J. Chem.* **2021**, *74*, 65–76.
- [54] R. Volpe, L. Aurelio, M. G. Gillin, E. H. Krenske, B. L. Flynn, *Chem. Eur. J.* **2015**, *21*, 10191–10199.
- [55] K. O. Hessian, B. L. Flynn, *Org. Lett.* **2006**, *8*, 243–246.
- [56] C. Zhou, A. v. Dubrovsky, R. C. Larock, *J. Org. Chem.* **2006**, *71*, 1626–1632.
- [57] X. Yu, J. Wu, *J. Comb. Chem.* **2009**, *11*, 895–899.
- [58] H. P. Zhang, H. Y. Li, H. F. Xiao, *J. Chem. Res.* **2013**, *37*, 556–558.
- [59] Q. Huang, J. A. Hunter, R. C. Larock, *J. Org. Chem.* **2002**, *67*, 3437–3444.
- [60] See the Supporting Information for the structural assignment of this compound using 2d nmr experiments.
- [61] A. L. Ruchelman, S. K. Singh, A. Ray, X. Wu, J. M. Yang, N. Zhou, A. Liu, L. F. Liu, E. J. LaVoie, *Bioorg. Med. Chem.* **2004**, *12*, 795–806.
- [62] T. Mitamura, A. Nomoto, M. Sonoda, A. Ogawa, *Bull. Chem. Soc. Jpn.* **2010**, *83*, 822–824.
- [63] Y. Pommier, A. Nussenzweig, S. Takeda, C. Austin, *Nat. Rev. Mol. Cell Biol.* **2022**, DOI 10.1038/s41580-022-00452-3.
- [64] F. Meng, X. Nguyen, X. Cai, J. Duan, M. Matteucci, C. P. Hart, *Anti-Cancer Drugs* **2007**, *18*, 435–445.
- [65] A. Rapisarda, B. Uranchimeg, O. Sordet, Y. Pommier, R. H. Shoemaker, G. Melillo, *Cancer Res.* **2004**, *64*, 1475–1482.
- [66] J. Schovaneck, P. Bullova, Y. Tayem, A. Giubellino, R. Wesley, N. Lendvai, S. Nörling, J. Kopecek, Z. Frysak, Y. Pommier, S. Kummur, K. Pacak, *Endocrinology* **2015**, *156*, 4094–4104.
- [67] Y. Pommier, M. Cushman, *Mol. Cancer Ther.* **2009**, *8*, 1008–1014.
- [68] T. S. Dexheimer, Y. Pommier, *Nat. Protoc.* **2008**, *3*, 1736–1750.
- [69] See the Supporting Information for the Biological Data of Test Compounds, n.d.
- [70] C. Marchand, S. Antony, K. W. Kohn, M. Cushman, A. Ioanoviciu, B. L. Staker, A. B. Burgin, L. Stewart, Y. Pommier, *Mol. Cancer Ther.* **2006**, *5*, 287–295.
- [71] Y. Pommier, E. Kiselev, C. Marchand, *Bioorg. Med. Chem. Lett.* **2015**, *25*, 3961–3965.
- [72] M. Satyanarayana, W. Feng, L. Cheng, A. A. Liu, Y. C. Tsai, L. F. Liu, E. J. LaVoie, *Bioorg. Med. Chem.* **2008**, *16*, 7824–7831.
- [73] L. Aurelio, C. v. Scullino, M. R. Pitman, A. Sexton, V. Oliver, L. Davies, R. J. Rebello, L. Furic, D. J. Creek, S. M. Pitson, B. L. Flynn, *J. Med. Chem.* **2016**, *59*, 965–984.

Manuscript received: June 22, 2022
Accepted manuscript online: September 7, 2022
Version of record online: November 3, 2022